Unsteady Transonic Flows Past Airfoils Using the Euler Equations

Gregory E. Smith*
North Carolina State University
Raleigh North Carolina

Woodrow Whitlow Jr.†
NASA Langley Research Center, Hampton, Virginia
and
H. A. Hassan‡
North Carolina State University
Raleigh, North Carolina

Introduction

TRANSONIC flow around oscillating airfoils is characterized by the presence of subsonic and supersonic flow regions and moving shock waves of varying strength. Determining the resulting aerodynamic forces is crucial in determining flutter speeds and in designing control systems needed for automatic pilots, stabilization of inherently unstable aircraft, spin prevention systems, maneuver and gust load alleviation, and flutter suppression. Many of the unsteady transonic calculations to date are based on the transonic small-disturbance potential equation. Solutions based on such equations are not accurate enough in the transonic region.[1] Moreover, they suffer from lack of uniqueness.[2] Use of the conservative full potential equation improves the accuracy, but lack of uniqueness remains a problem.

It has been shown recently by Salas and Gumbert[3] that the nonuniqueness problem of the full conservative potential model is a result of the breakdown of the model. Thus, in order to obtain usable solutions in this critical regime, one must modify the conservative full potential formulation in the manner suggested by Klopfer and Nixon[4] or Hafez and Lovell.[5] Such an approach was presented in Ref. 6. Another option is to use the Euler equations. This is the approach pursued here.

The Euler equations provide the correct description of inviscid flows in the transonic and all other flow regimes. The Euler code developed in this investigation employs an explicit time-stepping scheme based on a four-step Runge-Kutta method.[7] The conditions employed at inflow and outflow boundaries are determined from the time-dependent theory of characteristics.[8] Finally, the code incorporates a time-dependent, automatic grid generation procedure similar to that used by Chyu et al.[9] The resulting code was used to calculate steady and unsteady flows past two of the AGARD standard aeroelastic configurations: NACA 64A010 and NLR 7301 airfoils.

Received April 24, 1986; presented as Paper 86-1764 at the AIAA 4th Applied Aerodynamics Conference, San Diego, CA, June 9-11, 1986; revision received March 4, 1987.

*Research Assistant, Mechanical and Aerospace Engineering (presently with Technology Division, Dynamic Engineering Inc., Newport News, VA).

†Aerospace Engineer, Unsteady Aerodynamics Branch, Loads and Aeroelasticity Division. Member AIAA.

‡Professor, Mechanical and Aerospace Engineering. Associate Fellow AIAA.

Problem Formulation

The conservation law form of the dimensionless Euler equations in time-dependent curvilinear coordinates, i.e.,

$$\xi=\xi(x,y,t), \qquad \eta=\eta(x,y,t) \tag{1}$$

can be written as

$$\frac{\partial Q}{\partial t}+\frac{\partial F}{\partial \xi}+\frac{\partial G}{\partial \eta}=0 \tag{2}$$

where

$$Q=J[\rho,\rho u,\rho v,e]^T$$

$$F=J[\rho U,\rho uU+\xi_x p,\rho vU+\xi_y p,U(e+p)-\xi_t p]^T$$

$$G=J[\rho V,\rho uV+\eta_x p,\rho vV+\eta_y p,V(e+p)-\eta_t p]^T$$

$$J=x_\xi y_\eta - x_\eta y_\xi \tag{3}$$

In the above equation, ρ is the density, u and v the velocity components in the x and y directions, p the pressure, e the stagnation internal energy, and U and V are the contravariant velocities,

$$U=\xi_x u+\xi_y v+\xi_t, \quad V=\eta_x u+\eta_y v+\eta_t \tag{4}$$

A finite-difference method is used to solve the governing equations. Central difference operators are used in all directions. Because central difference schemes are not naturally dissipative, there is a need to add appropriate smoothing terms. These terms are generally of two types: a fourth-difference term to suppress odd-even point decoupling and a second-difference term to prevent oscillations in the vicinity of shock waves. The second-difference term causes the solution to be first-order accurate near a shock. The smoothing terms employed here are similar to those employed in Ref. 7. However, constant coefficients are employed in the current algorithm.

The boundary conditions are based on a procedure similar to that used by Whitfield and Janus.[8] Equation (2) can be written in the form

$$\frac{\partial Q}{\partial t}+A\frac{\partial Q}{\partial \xi}+B\frac{\partial Q}{\partial \eta}=0 \tag{5}$$

where A and B are 4×4 matrices defined as

$$A=\frac{\partial F}{\partial Q}, \qquad B=\frac{\partial G}{\partial Q} \tag{6}$$

The four simultaneous equations given by Eq. (5) are hyperbolic. Hence, each of the matrices A and B have four real eigenvalues that are the characteristic velocities in each of the spatial directions.

Equation (5) is the starting point of the derivation of the boundary conditions. As an illustration consider the boundary conditions at an $\eta=$ const boundary. For a locally one-dimensional flow, Eq. (5) reduces to

$$\frac{\partial Q}{\partial t}+A\frac{\partial Q}{\partial \xi}=0 \tag{7}$$

Because the matrix A has a complete set of eigenvalues and eigenvectors, a similarity transformation exists, which makes it possible to write A as

$$A=P\Lambda P^{-1} \tag{8}$$

where P is a matrix whose columns consist of the right eigenvectors of A and Λ a diagonal matrix consisting of the

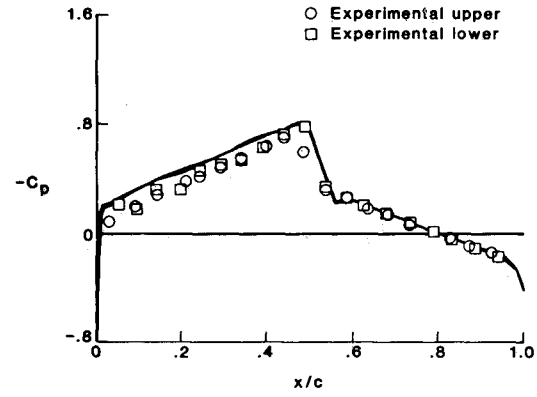

a) Steady pressure.

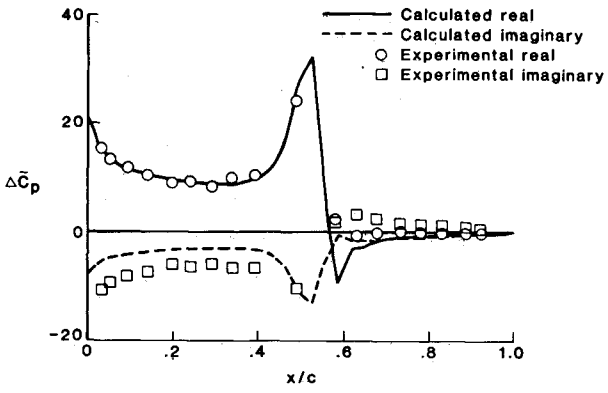

b) Unsteady lifting pressure.

Fig. 1 Pressure distributions for the NACA 64A010 airfoil.

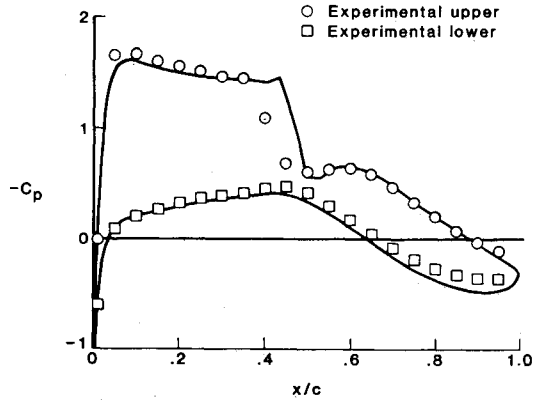

a) Steady pressure.

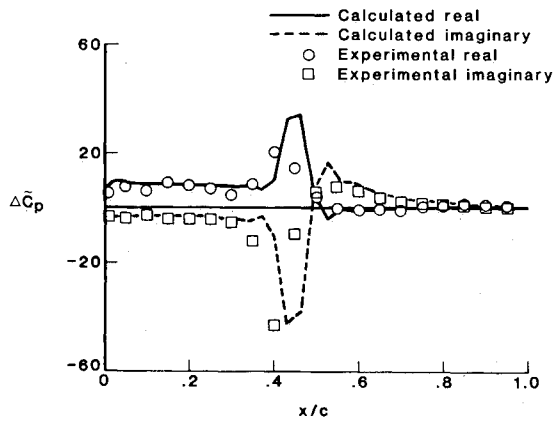

b) Unsteady lifting pressure.

Fig. 2 Pressure distributions for the NLR 7301 airfoil.

eigenvalues of A, i.e.,

$$\lambda_1,\lambda_2=\xi_x u+\xi_y v+\xi_t=U,\quad \lambda_3,\lambda_4=\lambda_1\pm a\,|\nabla\xi| \tag{9}$$

where a is the speed of sound. Multiplying Eq. (7) by P^{-1} and assuming that P^{-1} is locally constant, one finds

$$\frac{\partial w}{\partial t}+\Lambda\frac{\partial w}{\partial \xi}=0,\qquad w=P^{-1}Q \tag{10}$$

Equation (10) provides the necessary boundary condition at an $\eta=$ constant boundary. A similar approach is used at a $\xi=$ constant boundary.

Upwind differencing is used to replace the spatial derivatives in Eq. (10). The same time-stepping scheme used to integrate the governing equations is used to integrate Eq. (10) and similar boundary conditions at $\eta=$ constant boundaries. At the airfoil surface

$$V=0 \tag{11}$$

which results in the vanishing of two eigenvalues there. Therefore, the above general approach for handling conditions at free boundaries is not appropriate for solid surfaces. Thus, Eq. (11) is enforced at the airfoil boundary. Other parameters needed there were obtained by extrapolation.

All computations reported here employed C grids. The grids were generated by two different procedures. The first employed the GRAPE routine of Steger and Sorenson,[10] which is based on an elliptic solver. The second is an algebraic grid generation method. For oscillating airfoils, these routines were used to generate grids at the extreme angles of attack. The grids were stored and the interpolation procedure of Ref. 9 was then used to update the grid at each time step.

A modified four-step Runge-Kutta integration scheme[7] is employed to integrate Eqs. (2) and (10). The (dimensionless) time step Δt is calculated using a procedure similar to that of MacCormack[11]

$$\Delta t=\frac{\mathrm{CFL}}{U+V+a(\,|\nabla\xi|+|\nabla\eta|\,)} \tag{12}$$

where the Courant number CFL is 1 for points on the boundary and $2\sqrt{2}$ for interior points. When calculating steady-state flows, the solution is advanced in time with a local time step given by Eq. (12). This practice allows faster signal propagation and thus faster convergence. For the unsteady solutions, the solution is advanced in time using the minimum Δt given by Eq. (12). This is why time-accurate calculations are costly.

Results and Discussion

The results presented here are intended to demonstrate the importance of using the Euler equations in situations where potential flow theories are not accurate. Calculations were carried out for two airfoils. In order to check the accuracy of the method calculations were carried out first for an NACA 64A010. Flows past this airfoil are well predicted by the transonic small-disturbance equation.[1] The other airfoil is the NLR 7301. For pitch about a mean angle of attack α_m, the total angle of attack is represented as

$$\alpha(t)=\alpha_m+\alpha_0\sin\omega t,\quad \omega=2kU_\infty/c$$

where α_0 is the dynamic pitch angle, k the reduced frequency, U_∞ the freestream velocity, and c the chord length.

For each of the configurations considered the steady pressure coefficient is presented. In addition, for each of the time-dependent cases, the first harmonic of the lifting pressure coefficients (lower minus upper) is given. The unsteady pressures are calculated as real (in-phase) and imaginary (in-quadrature) parts of the first harmonic component of the pressure. The harmonic components are normalized by the nondimensional amplitude of motion in radians and calculated for the last cycle of imposed harmonic motion using a fast Fourier transform analysis. All results presented here were calculated using 140×40 C grids.

Figure 1a shows the steady pressure distribution for an NACA 64A010 airfoil at a freestream Mach number $M = 0.796$ and angle of attack $\alpha_m = 0$ deg. Figure 1b shows the lifting pressure coefficient for $k = 0.101$, pitch axis location relative to leading edge $x_\alpha/c = 0.25$, and $\alpha_0 = 1.02$ deg. The case considered here is for the model tested at the NASA Ames Research Center.[12] Figure 2 shows similar results for the NLR 7301 airfoil at $M = 0.7$, $\alpha_m = 2.0$ deg, $k = 0.192$, $x_\alpha/c = 0.4$, and $\alpha_0 = 0.5$ deg. Because of limited computer resources, the unsteady results were marched in time for two cycles of harmonic motion. In spite of this, good agreement between theory and experiment is indicated. In general, when the steady-state solution agrees with experiment, the unsteady results behave similarly if the solution is marched in time until all of the transients disappear. Better agreement is indicated in Figs. 1b and 2b with the real part of $\Delta \bar{C}_p$. Evidently, the imaginary part is more dependent on the speed and location of the shock. Because the calculations do not take viscous effects or wall interference effects into consideration, one should not expect to calculate the correct speed and position of the shock for oscillating airfoils. Thus, it may be necessary to include viscous effects for calculations of flutter boundaries, etc., in transonic flow.

In conclusion, the results presented here show that calculations based on the Euler equations are reliable enough so that they may be used to calculate flutter boundaries and other information needed for active flutter suppression, gust load alleviation, etc. However, in regions where viscous-inviscid interactions are important, the Euler equations must be coupled with the boundary-layer equations.

Acknowledgment

The authors would like to acknowledge many helpful discussions with Robert N. Desmarais, David A. Seidel, and Drs. Robert M. Bennett, Samuel R. Bland, and John W. Edwards of the NASA Langley Research Center. The work was supported in part by NASA Grant NGT 34-002-800.

References

[1]Bland, S. R. and Seidel, D. A., "Calculation of Unsteady Aerodynamics for Four AGARD Standard Aeroelastic Configurations," NASA TM 85817, May 1984.

[2]Dowell, E. H., Ueda, T., and Goorjian, P. M., "Transient Decay Times and Mean Values of Unsteady Oscillations in Transonic Flow," *AIAA Journal*, Vol. 21, Dec. 1983, pp. 1762–1764.

[3]Salas, M. D. and Gumbert, C. R., "Breakdown of the Conservative Potential Equation," AIAA Paper 85-0367, Jan. 1985.

[4]Klopfer, G. H. and Nixon, D., "Non-Isentropic Potential Formulation for Transonic Flows," AIAA Paper 83-0375, Jan. 1983.

[5]Hafez, M. M. and Lovell, D., "Entropy and Vorticity Correction for Transonic Flows," AIAA Paper 83-1926, July 1983.

[6]Whitlow, W. Jr., Hafez, M. M., and Osher, S. J., "An Entropy Correction Method for Unsteady Full Potential Flows with Strong Shocks," AIAA Paper 86-1768, June 1986.

[7]Jameson, A. and Baker, T. J., "Solution of the Euler Equations for Complex Configurations," AIAA Paper 83-1929, July 1983.

[8]Whitfield, D. L. and Janus, J. M., "Three-Dimensional Unsteady Euler Equations Solution Using Flux Vector Splitting," AIAA Paper 84-1552, June 1984.

[9]Chyu, W. J., Davis, S. S., and Chang, K. S., "Calculation of Unsteady Transonic Flow over an Airfoil," *AIAA Journal*, Vol. 19, June 1981, pp. 684-690.

[10]Steger, J. L. and Sorenson, R. L., "Automatic Mesh Point Clustering Near a Boundary in Grid Generation with Elliptic Partial Differential Equations," *Journal of Computational Physics*, Vol. 33, Dec. 1979, pp. 405–410 (also Sorenson, R. L., NASA TM 81198, May 1980).

[11]MacCormack, R. W., "Numerical Solution of the Interaction of a Shock Wave with a Laminar Boundary Layer," *Lecture Notes in Physics*, Vol. 8, Springer-Verlag, New York, 1971, pp. 151–163.

[12]Davis, S. and Malcom, G., "Experimental Unsteady Aerodynamics of Conventional and Supercritical Airfoils," NASA TM 81221, Aug. 1980.